

# Effect of fabrication errors on multiple second-harmonic generation considering pump depletion

Qiushuang Zhao (赵秋爽) and Liming Zhao (赵丽明)\*

Center for Theoretical Physics, Department of Physics, Capital Normal University,  
Beijing 100048, China

\*Corresponding author: me\_zlm@sohu.com

Received September 23, 2014; accepted December 22, 2014; posted online January 27, 2015

We investigate second-harmonic generation (SHG) from aperiodic optical superlattices in the regime of pump depletion, where the influence of typical fabrication errors which can be introduced by the random fluctuation of the thickness for each domain in the simulation is considered according to the actual case. It is found that both the SHG conversion efficiencies calculated in undepleted pump approximation (UPA) and an exact solution decrease when the fluctuation gets larger. However, the decreasing degree is related to the wavelength of the fundamental wave (FW), and the longer the FW wavelength, the lesser the corresponding conversion efficiency reduction. A relative tolerance with respect to SHG conversion efficiency calculated in UPA and exact solution is defined in a previous work, in which a typical model based on the relative tolerance curves is proposed to estimate the SHG conversion efficiency. The simulation results exhibit that the relative tolerance curves are basically coincident with the standard curve when the random fluctuation is very small (typically below 1%). However, as the fluctuation increases, the relative tolerance curves exhibit a large deviation from the standard one, and the deviation is also determined by the wavelength of the FW.

OCIS codes: 050.5298, 120.5060, 130.4310, 130.7405.

doi: 10.3788/COL201513.S10501.

Using an electric poling technique for domain inversion in ferroelectric crystals, the quasi-phase matching (QPM)<sup>[1,2]</sup> has been extensively used in various superlattices, including the periodic<sup>[3,4]</sup>, quasi-periodic<sup>[5-7]</sup>, nonperiodic<sup>[8]</sup> optical superlattice, aperiodic optical superlattice (AOS)<sup>[9-12]</sup>, and disorder domain configuration<sup>[13,14]</sup>. Note that all these structures aim at obtaining good phase matching and enhancing the optical frequency conversion, mostly focusing on second-harmonic generation (SHG). It is well-known that QPM is obtained under the undepleted pump approximation (UPA). However, when the conversion efficiency of SHG is high enough, the depletion of the fundamental wave (FW) cannot be ignored. Based on this case, more attention is focused on achieving compact and high-power laser pulses via SHG taking pump depletion<sup>[15-20]</sup> into account. Recently, Zhao *et al.* reported the application of multiple QPM grating designed in UPA for SHG in the regime of pump depletion. The results show that the AOS sample devised in UPA applies to a general situation of low and high conversion efficiencies of SHG, and a practical sample can be accurately evaluated by a developed model which can be shown by a relative tolerance curve, called the standard curve in this letter. The relative tolerance is based on the SHG conversion efficiency calculated in UPA and exact solution, which is determined only by the conversion efficiency with no relation to the pump intensity, pre-assigned wavelength, sample configuration, and the nonlinear media.

For the AOS configuration, samples are divided into layers<sup>[21]</sup> arranging as alternating orientation of

polarization, and the width of individual domain is optimized by simulated annealing (SA) algorithm. However, fabrication errors inevitably exist and should be considered for an actual sample. The results for the perfect AOS sample are provided in Ref. [18], however, whether the conclusion proposed by Zhao *et al.*<sup>[18]</sup> are still valid with the typical fabrication errors has to be considered for realistic application. That is to say, how the random fluctuation impacts on the conversion efficiency of SHG in UPA and exact solution; whether a relative tolerance curve will be deviated from the standard curve is still in question. In this letter, we focus on investigating the above issues. We start with theoretical model for necessary formulae used in calculations, the simulation results are presented with analyses subsequently and conclude with a brief summary.

Firstly, we discuss a one-dimensional AOS sample made by LiNbO<sub>3</sub> crystal layers, the directions of polarization vectors in successive domains are opposite as are signs of nonlinear optical coefficients. However, the width of each layer may be determined by the specified optical parametric processes. Each domain is parallel to the *yz* plane, and the propagation and the polarization directions of incident light are along the *x* and *z* axes, respectively. In the AOS sample, a FW  $\omega_1 = \omega$  is perpendicularly incident onto the surface, and the second-harmonic wave (SHW) with  $\omega_2 = 2\omega$  is generated by nonlinear optical process. In the assumption of slowing wave variation of field amplitudes, the equations governing the propagation of the FW and the SHW are

$$\frac{dE_1(x)}{dx} = \frac{i\omega_1^2 \chi^{(2)}(x)}{k_1 c^2} E_2(x) E_1^*(x) e^{i\Delta k x}, \quad (1a)$$

$$\frac{dE_2(x)}{dx} = \frac{i\omega_2^2 \chi^{(2)}(x)}{2k_2 c^2} E_1^2(x) e^{-i\Delta k x}, \quad (1b)$$

where  $k_1 = n_1 \omega/c$  ( $k_2 = 2n_2 \omega/c$ ),  $c$  is the speed of light in vacuum,  $n_1$  ( $n_2$ ) is the refractive index of the material at the FW (SHW) frequency, and  $\Delta k = k_2 - 2k_1$  denotes the wave vector mismatch between FW and SHW. In the designation, we use

$$\chi_2(x) = 2 |d_{33}| \tilde{d}(x), \quad (2)$$

where  $\tilde{d}(x)$  (taking a binary value of 1 or  $-1$ ) represents the spatial distribution of domain orientation. Since the field can be written in its real and imaginary parts  $E_a(x) = \rho_a(x) e^{i\phi_a(x)}$  ( $a = 1, 2$ ), the variable replacement is

$$u_a(x) = \left( \frac{\varepsilon_0 c^2 k_a}{2\omega_a I} \right)^{1/2} \rho_a(x), \quad a = 1, 2, \quad (3)$$

where  $u_a^2(x)$  represents the normalized intensity,  $L$  is the length of the sample. The conversion efficiency is given by

$$\eta = u_2^2(L). \quad (4)$$

Via several substitutions and integrals similar to Ref. [18], the exact solution  $u_2(x_n)$  can be obtained as long as the domain configuration is given. Thus, the corresponding conversion efficiency can be achieved after the AOS sample is constructed.

We adopt the following parameters in the designation of the AOS as follows: the pre-assigned FW wavelengths are  $\lambda_1 = 0.972 \mu\text{m}$ ,  $\lambda_2 = 1.064 \mu\text{m}$ , and  $\lambda_3 = 1.283 \mu\text{m}$ . The number of domains  $N = 1800$ , and the thickness of a single domain  $\Delta x = 3 \mu\text{m}$ . We set the intensity of the incident light waves as  $I = 1.0 \times 10^{11} \text{ W/m}^2$  and  $d_{33} = 27.0 \text{ pm/v}$ . An AOS sample which can achieve the above three wavelengths with high enough and nearly identical conversion efficiency of SHG is designed by the SA algorithm in UPA. We impose a random distribution function  $aa$  in the range of  $[0, 1]$  on the thickness of each block. Therefore, the thickness of the  $i$ th block in an actual sample can be written as  $dx(i) = \Delta x + (aa - 0.5)/0.5 * \Delta x * \delta$  in our simulation. Here  $\Delta x = 3 \mu\text{m}$  is the thickness of every block adopted in the perfect AOS sample. It can be deduced that  $\delta$  stands for the range of fabrication errors and  $0 \leq \delta \leq 1$ . For example,  $\delta = 0.01$  means  $\Delta x$  taking 1% random fluctuation around its accuracy, thus  $\frac{dx(i) - \Delta x}{\Delta x}$

will be in the range of  $[-0.01, 0.01]$ . The conversion efficiency for exact solution as a function of wavelength with different random fluctuations  $\delta$  is displayed in Fig. 1. The black curve is obtained from the devised AOS sample and the fabrication errors are not considered. While the fabrication errors are considered for the other curves, the

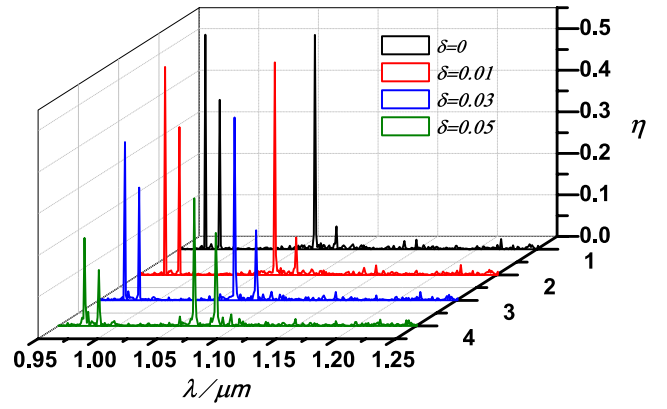


Fig. 1. Variation of SHG conversion efficiency  $\eta$  for exact solution with the wavelength for different  $\delta$ . The black, red, blue, and green curves represent  $\delta = 0, 0.01, 0.03$ , and  $0.05$ , respectively.

red, blue, and green curves represent  $\delta = 0.01, 0.03$ , and  $0.05$ , respectively. It is found that for the black curve,  $\eta$  exhibits significant uniformity for the three pre-assigned wavelengths, except for the two unexpected peaks with  $\lambda = 0.984$  and  $1.082 \mu\text{m}$  appearing in the vicinity of  $\lambda_1$  and  $\lambda_2$ , which denotes that the AOS sample can also achieve high and nearly coincident SHG conversion efficiency for an exact solution. For the other curves, the high conversion efficiency can also be achieved for the preset multiple wavelengths. However, the uniformity of the peak values is destroyed and the corresponding peak values are decreased with increasing  $\delta$ . For example, when  $\delta = 3\%$ , the  $\eta$  for  $\lambda_1$  reduces from 0.52 to 0.38, changing about 26%; for  $\lambda_3$ , it varies from 0.52 to 0.48, decreasing about 6%. It is found that the longer wavelength suffers from lesser reduction in SHG conversion efficiency, which leads to the inconsistency of the peak values.

In order to further reveal the characteristic of the SHG in the constructed AOS with the consideration of fabrication errors, the variation of exact solution with the sequence of domain for different random fluctuations  $\delta$  at the three wavelengths are shown in Fig. 2(a) for  $\lambda_1 = 0.972 \mu\text{m}$ , Fig. 2(b) for  $\lambda_2 = 1.064 \mu\text{m}$ , Fig. 2(c) for  $\lambda_3 = 1.283 \mu\text{m}$ ,

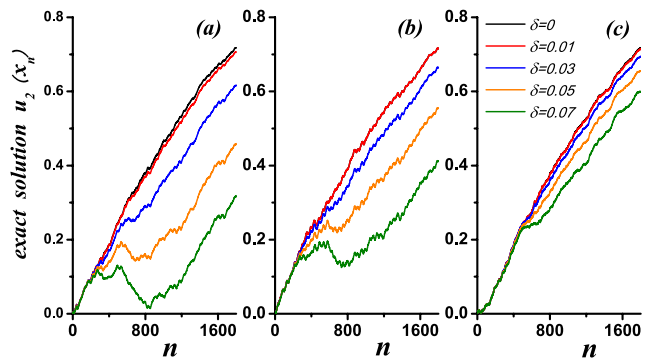


Fig. 2.  $u_2(x_n)$  versus the sequence of domain  $n$  for the pre-assigned wavelengths under different  $\delta$ : (a) 0.972, (b) 1.064, and (c) 1.283  $\mu\text{m}$ . The black, red, blue, orange, and green curves represent  $\delta = 0, 0.01, 0.03, 0.05$ , and  $0.07$ , respectively.

and the black, red, blue, orange, and green curves denote the case of  $\delta = 0, 0.01, 0.03, 0.05,$  and  $0.07,$  respectively. For the black curve,  $u_2(x_n)$  is monotonically increasing with  $n$ , which implies that the contribution of the individual block on SHG process is positive, and the good phase matching between FW and SHW can be achieved in the perfect AOS sample. However, when the random fluctuation is introduced and becomes larger and larger (especially beyond 3%), the variation of  $u_2(x_n)$  appears to be oscillating and the oscillation behavior grows more severe with increasing  $\delta$ . For example in Fig. 2(a),  $u_2(x_n)$  exhibits a dramatic decrease at  $n = 500$ , then begins to increase when  $n = 800$ . The same case is shown for  $\lambda = 1.064 \mu\text{m}$ , whereas for  $\lambda = 1.283 \mu\text{m}$ , the oscillation is much weaker. These results obtained here indicate that the random fluctuation leads to the phase mismatch between the FW and SHW. Moreover, the phase mismatch is also related to wavelength, and the shorter the wavelength, the stronger the mismatch between the FW and SHW. This conclusion is also consistent with the fact obtained from Fig. 1 that the  $\eta$  for  $u_2$  shows less decrease for the longer wavelength with the same  $\delta$ .

In Ref. [18], a relative tolerance is defined as  $\sigma = \frac{\tilde{u}_2(x_n) - u_2(x_n)}{u_2(x_n)}$  to evaluate the difference of SHG between UPA and an exact solution. Here  $\tilde{u}_2(x_n)$  refers to the value calculated in UPA. It is found that the relative tolerance is solely determined by the SHG conversion efficiency, but unrelated to the sample configuration, the nonlinear media, and the incident intensity. A model to assess  $u_2(x_n)$  was assumed as

$$\sigma = 0.39u_2^2(x_n) - 0.0115u_2(x_n) \quad (u_2(x_n) \leq 0.4), \quad (5a)$$

$$\sigma = 0.0097e^{u_2(x_n)/0.217} \quad (0.4 < u_2(x_n) < 0.9). \quad (5b)$$

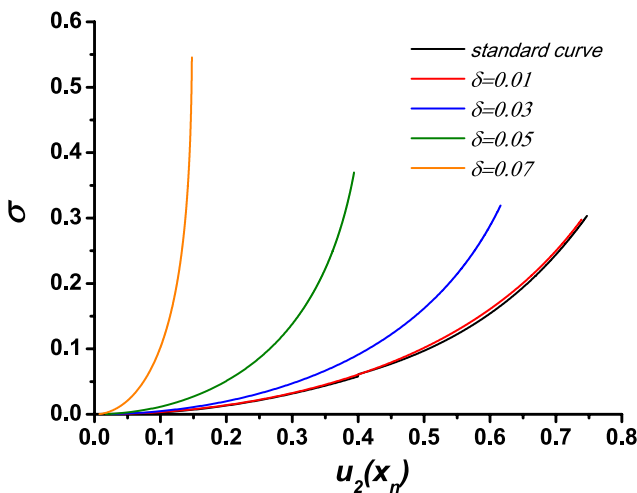


Fig. 3. Variation of  $\sigma$  as a function of  $u_2(x_n)$  for  $\lambda = 0.972 \mu\text{m}$ . The black curve is the standard curve according to Eq. (5) and the red, blue, green, and orange curves denote the data for  $\delta = 0.01, 0.03, 0.05,$  and  $0.07,$  respectively.

The model itself proves easy and convenient to estimate the SHG conversion efficiency when pump depletion cannot be ignored. However, Eq. (5) is fitted for the case of the perfect AOS configuration, and for an actual sample, fabrication errors are inevitably involved. We now proceed to discuss whether the developed model is fitted for the case when fabrication errors are introduced in an actual AOS sample. Figure 3 shows the variation of  $\sigma$  versus  $u_2(x_n)$  under different  $\delta$  for  $\lambda_1 = 0.972 \mu\text{m}$ . The black curve represents the standard curve which can be obtained for Eq. (5), and the other red, blue, green, and orange curves stand for the case of  $\delta = 0.01, 0.03, 0.05,$  and  $0.07,$  respectively. It is clearly observed that the curves are inclined to deviate from the standard curve with increasing  $\delta$ , except for  $\delta = 0.01$ , which is nearly coincident with the black curve. There appears higher deviation with increasing  $\delta$ . Note that the deviation of a relative tolerance curve from the standard one is related to the FW wavelength. Figure 4 shows the relative tolerance curves for different FW wavelengths when  $\delta$  is set to 5%. The black curve is the standard curve, and the red, blue, and green curves successively correspond to  $\lambda = 1.283, 1.064,$  and  $0.972 \mu\text{m}$ . Clearly, for  $\lambda = 0.972 \mu\text{m}$ , the relative tolerance curve displays serious deviation from the standard curve, whereas the departure degree is much smaller for  $\lambda = 1.283 \mu\text{m}$ .

In conclusion, we redraw the outcome obtained from an earlier work where the random fluctuation of the thickness of each block in AOS is introduced due to the inevitable existence of fabrication errors in an actual sample. The results show that both the conversion efficiencies calculated in UPA and an exact solution are decreasing with increasing random fluctuation, and the decreasing degree is related to the FW wavelength. The longer wavelength suffers from lesser reduction. A relative

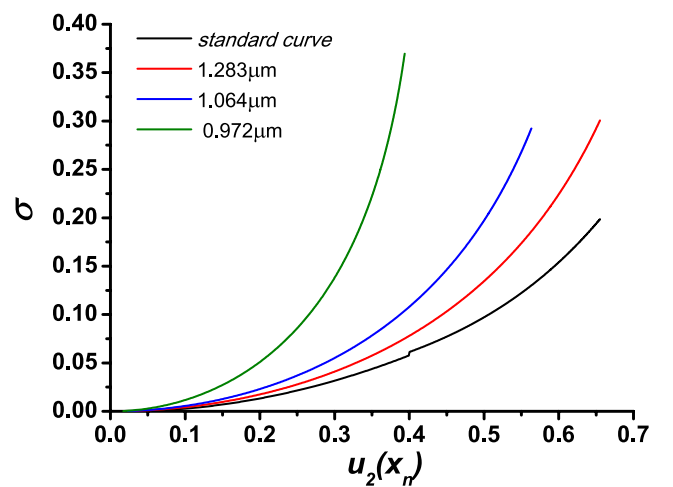


Fig. 4. Relative tolerance  $\sigma$  with respect to  $u_2(x_n)$  for different FW wavelengths under 5% random fluctuation. The black curve is the standard curve according to Eq. (5) and the red, blue, and green curves denote the data for  $\lambda = 1.283, 1.064,$  and  $0.972 \mu\text{m}$ , respectively.

tolerance based on UPA and an exact solution is calculated under different random fluctuations. It is found that the relative tolerance curves coincident with the standard curve only when the random fluctuation is very small (typically below 1%), and then exhibit more and more serious deviation with increasing  $\delta$ . Moreover, the deviation degree is also related to the FW wavelength, the longer wavelength is closer to the standard curve.

This work was supported by the National Natural Science Foundation of China (Nos. 11274233 and 11004139) and the Natural Science Foundation of Beijing (No. 1102012).

## References

1. A. Armstrong, N. Bloembergen, J. Ducuing, and P. S. Pershan, *Phys. Rev.* **127**, 1918 (1962).
2. N. Bloembergen and A. J. Sievers, *Appl. Phys. Lett.* **17**, 483 (1970).
3. Y. Chen, J. Zhang, and H. Li, *Chin. Opt. Lett.* **11**, 031601 (2013).
4. B. F. Johnston, P. Dekker, S. M. Saltiel, Y. S. Kivshar, and M. J. Withford, *Opt. Express* **15**, 13630 (2007).
5. Y. Y. Zhu, Y. Q. Qin, C. Zhang, S. N. Zhu, and N. B. Ming, *J. Phys.* **12**, 10639 (2000).
6. R. Lifshitz, A. Arie, and A. Bahabad, *Phys. Rev. Lett.* **95**, 133901 (2005).
7. B. Ma, M. Ren, and Z. Li, *Chin. Opt. Lett.* **10**, S21904 (2012).
8. X. F. Chen, F. Wu, X. L. Zeng, Y. P. Chen, Y. X. Xia, and Y. L. Chen, *Phys. Rev. A* **69**, 013818 (2004).
9. M. A. Arbore, O. Marco, and M. M. Fejer, *Opt. Lett.* **22**, 865 (1997).
10. Y. W. Lee, F. C. Fan, Y. C. Huang, B. Y. Gu, and B. Z. Dong, *Opt. Lett.* **27**, 2191 (2002).
11. X. Gu, X. F. Chen, Y. P. Chen, X. L. Zeng, Y. X. Xia, and Y. L. Chen, *Opt. Commun.* **237**, 53 (2004).
12. L. J. Chen, X. F. Chen, Y. P. Chen, and Y. X. Xia, *Phys. Lett. A* **349**, 484 (2006).
13. X. Vidal and J. Martorell, *Phys. Rev. Lett.* **97**, 013902 (2006).
14. R. Fischer, S. M. Saltiel, D. N. Neshev, W. Krolikowski, and Y. S. Kivshar, *Appl. Phys. Lett.* **89**, 191105 (2006).
15. L. M. Zhao, G. K. Yue, and Y. S. Zhou, *Europhys. Lett.* **99**, 34002 (2012).
16. L. M. Zhao, B. Y. Gu, G. Z. Yang, and Y. S. Zhou, *J. Nonlinear Opt. Phys. Mater.* **14**, 115 (2005).
17. R. Buffa and S. Cavalieri, *J. Opt. Soc. Am. B* **17**, 1901 (2000).
18. L. M. Zhao, G. K. Yue, Y. S. Zhou, and F. H. Wang, *Opt. Express* **21**, 17592 (2013).
19. U. K. Sapaev and G. Assanto, *Opt. Express* **15**, 7448 (2007).
20. J. H. Yuan, J. Yang, W. B. Ai, and T. P. Shuai, *Opt. Commun.* **315**, 381 (2014).
21. J. Jones, L. Zhu, N. Tolk, and R. Mu, in *MRS Online Proceedings Library* 912 (2013).